MD and BCA simulations of He and H bombardment of fuzz in bcc elements

Klaver, Peter; Zhang, S.; Nordlund, K.

DOI
10.1016/j.jnucmat.2017.05.023

Publication date
2017

Document Version
Final published version

Published in
Journal of Nuclear Materials

Journal of Nuclear Materials 492 (2017) 113–121

Contents lists available at ScienceDirect

Journal of Nuclear Materials

journal homepage: www.elsevier.com/locate/jnucmat

MD and BCA simulations of He and H bombardment of fuzz in bcc elements

T.P.C. Klaver [a, b, *], S. Zhang [c, d], K. Nordlund [c]

[a] FOM Institute DIFFER - Dutch Institute for Fundamental Energy Research, Partner in the Trilateral Euregio Cluster, Eindhoven, The Netherlands
[b] Department of Materials Science and Engineering, Delft University of Technology, Delft, The Netherlands
[c] Department of Physics, University of Helsinki, Helsinki, Finland
[d] School of Nuclear Science and Technology, Lanzhou University, Lanzhou, China

ARTICLE INFO

Article history:
Received 16 November 2016
Received in revised form
17 May 2017
Accepted 17 May 2017
Available online 19 May 2017

ABSTRACT

We present results of MD simulations of low energy He ion bombardment of low density fuzz in bcc elements. He ions can penetrate several micrometers into sparse fuzz, which allows for a sufficient He flux through it to grow the fuzz further. He kinetic energy falls off exponentially with penetration depth. A BCA code was used to carry out the same ion bombardment on the same fuzz structures as in MD simulations, but with simpler, 10 million times faster calculations. Despite the poor theoretical basis of the BCA at low ion energies, and the use of somewhat different potentials in MD and BCA calculations, the ion penetration depths predicted by BCA are only ~12% less than those predicted by MD. The MD-BCA differences are highly systematic and trends in the results of the two methods are very similar. We have carried out more than 200 BCA calculation runs of ion bombardment of fuzz, in which parameters in the ion bombardment process were varied. For most parameters, the results show that the ion bombardment process is quite generic. The ion species (He or H), ion mass, fuzz element (W, Ta, Mo, Fe) and fuzz element lattice parameter turned out to have a modest influence on ion penetration depths at most. An off-normal angle of incidence strongly reduces the ion penetration depth. Increasing the ion energy increases the ion penetration, but the rate by which ion energy drops off at high ion energies follows the same exponential pattern as at lower energies.

1. Introduction

Plasma facing materials for future fusion energy reactors continue to be an active field of research. The expected formation of low density W 'fuzz' on the divertor has received wide attention (see references 2–28 in Ref. [1]) since the first reporting [2] of W fuzz formation under circumstances similar to those in a fusion reactor. The formation of fuzz on other metals and its potential application in water splitting [e.g. 3, 4] has fuelled further interest. Recently, we published [1] molecular dynamics (MD) simulation results suggesting that the transport of He through the fuzz to the W bulk, which is required for further growth 'from the bottom' of the fuzz, takes place ballistically, i. e. He ions move mostly freely through the open space in the fuzz, occasionally bouncing off the surface of a W nanorod. We found that the fraction of open channels in the fuzz through which ions can travel unimpeded is by far the most important parameter determining how deep ions penetrate into the fuzz. Furthermore, we found that the ability of ions to penetrate into the W drops off exponentially with penetration depth, meaning that He ion penetration into fuzz can be characterized by a 'half depth'. It was shown that the ion penetration in fuzz is qualitatively different from that in bulk, with ion penetration depths orders of magnitude deeper than in a homogeneous material of the same density. The fuzz structures in our previous work had ~15 vol-% W and had half depths of only a few hundred nm at most. Half depths for fuzz structures of much lower density, as were recently reported [5], might be measured in μm. If that would prove to be the case, ballistic He penetration might provide an adequate explanation for how He is supplied to the underlying W bulk through even the thickest fuzz layers grown so far.

In this paper we first present work that is an extension to lower density fuzz of our previous work. In section 2 we describe the

* Corresponding author.
E-mail address: klaver2@gmail.com (T.P.C. Klaver).

http://dx.doi.org/10.1016/j.jnucmat.2017.05.023
0022-3115/

creation of fuzz structures with W volume fractions from 11.0% down to 3.7%, the latter being close to recently reported experimental results [5]. As in our previous work, we work around the current inability of atomistic simulations to produce fuzz from bulk W by creating fully formed fuzz structures out of ellipsoids. After reporting computational details in section 3, we first present results of MD simulations of He bombardment of the 3.7–11.0 vol-% fuzz structures in section 4, showing that half depths can indeed reach μm's. We then show bombardment results for the same fuzz structures carried out with simpler BCA calculations, that require ~10 million times less cpu time. Having shown that the BCA calculations produce results acceptably close to MD simulations, we then show selected results of over 200 BCA calculation runs that were carried out to determine the influence of a number of parameters in the ion bombardment process. The parameters investigated were the ion species, ion mass, fuzz element, fuzz element lattice parameter, ion energy, and angle of incidence. In section 5 we discuss the implications of our results and a summary and conclusions are presented in section 6.

2. Creating W fuzz for He bombardment MD simulations

For MD calculations of He bombardment of fuzz an atom by atom description of a three dimensional fuzz structure is required as input. As far as we are aware, nobody has reported results of an experimental three dimensional structure determination of W fuzz. Hence we create our own fuzz structure with the right W volume fraction and with features with diameters as shown in TEM micrographs, as we did previously [1]. Ellipsoids provide the curved, rounded surfaces that nanorods would acquire at high temperature through surface diffusion, to reduce surface energy. Since many different ellipsoidal fuzz structure with the right W volume fraction and feature sizes can be created, one particular choice for how to create the structure need not be very similar to experimental fuzz. Hence we previously created a variety of structures, bombarded all of them with He and checked how much the differences between the structures influenced He penetration. Results showed that the shape and large scale surface roughness of fuzz building blocks are not decisive for the end results [1]. Texturing of the ellipsoids, to match the texture of nanorods shown in various TEM micrographs of fuzz, increases the amount of open channels (directions along which there are no W atoms at all, and along which He ions can move unimpeded in a straight line) perpendicular to the surface, through which ions can move unimpeded. This was shown to be by far the most important parameter governing ion penetration depth into fuzz. Therefore we varied only this parameter by building textured and randomly oriented fuzz structures out of ellipsoidal pieces of bcc W with smooth surfaces. Texturing of the fuzz structures is done by reducing the angle between the surface normal and the long axes of the ellipsoids by half, making the ellipsoids 'stand up more straight'. We built fuzz structures with a lower W volume fraction than in our previous work by creating a comparable number of ellipsoids (60, compared to 90 in previous work) in systems of larger volume. Systems with 3.67, 7.35 and 11.02 vol-% W were created. The in-plane dimensions of the 3.67 vol-% systems were 200 × 200 nm^2 and the fuzz thickness (z-direction) was 2.34 μm. Systems with 7.35 and 11.02 vol-% W were created by placing the centres of mass of ellipsoids at the same fractional coordinates within the supercells as for the 3.67 vol-% systems, but within smaller systems. The linear dimensions of the 7.35 and 11.02 vol-% systems were approximately $1/2^{1/3}$ and $1/3^{1/3}$ times those of the 3.67 vol-% systems, at 158 × 158 nm^2 x 1.86 μm and 138 × 138 nm^2 x 1.61 μm. The orientations of the ellipsoids were similar for all three W volume fractions.

In our previous work all ellipsoids were 20 nm wide and 63 nm long (ratio $1:\sqrt{10}$). In this work, ellipsoids have the same length/width ratio but the widths are a mixture of 20, 30, 40 and 50 nm, which corresponds more closely with experiments. As in our previous MD work, ellipsoids were hollowed out to shells of 2 nm or thicker, to reduce the number of atoms and thereby shorten computing time. Hollowing out the ellipsoids reduced the numbers of atoms from ~211 million to ~60 million. Table 1 provides information about the numbers of different sized dumbbells and atoms in the fuzz structures.

The centres of mass of 72 ellipsoids with different sizes were chosen randomly. To obtain a more even density distribution, a few large ellipsoids were moved to positions of smaller ones. Also, in areas of high density 10 smaller ellipsoids were deleted. The amount of open channels in the z-direction that resulted from the slightly tweaked density distribution is shown in Fig. 1 for textured and randomly oriented 3.67 vol-% fuzz. The percentage of open channels is determined for a structure such as shown on the left in Fig. 2 simply by determining the percentage of white pixels in the picture. Except for one dense part at ~40% of the fuzz thickness below the surface, the amount of open channels does not vary much. This means that for the fuzz structures we created, ion energy should fall off mostly exponentially, as we found previously [1].

Where there was overlap between two ellipsoids, the atoms of one of the ellipsoids in the overlapping volume were deleted. This slightly reduced the numbers of atoms, from 211 million to 206 million for the solid system with the most overlap. For each ellipsoid, the positions of a few W atoms were kept fixed. These fixed atoms served as anchor points, to keep ellipsoids from drifting. Fig. 2 shows an example of one of the fuzz structures.

3. Computational details

3.1. W/He MD simulations

The MD simulations in this work are a straightforward extension to lower fuzz volume fractions of our earlier work [1]. Most settings were similar. Table 2 lists the interatomic potentials used [6], along with their cut-off radii.

We used the potentials without electronic stopping. The Juslin-Wirth potential does not distinguish between charged or neutral He particles. We used the LAMMPS code for MD simulations [7]. In each fuzz system 10000 He ions were introduced with ~59 eV kinetic energy, under 0–7.1° off-normal angles. A variable time step was used to allow the fastest atom to move no more than 0.025 Å, which resulted in ~0.047 fs steps.

There are some differences related to the systems in the present work being nearly twice as big in terms of the number of atoms and 4 to 13 times bigger in terms of volume. It takes longer for He ions to lose their kinetic energy in larger, sparser systems, where collisions with surfaces are less frequent. Simulations were kept running until more than 98% of He ions had their kinetic energy reduced to 12 eV or less (compared to a threshold of less than 8 eV in our previous work). Despite allowing more He ions to have kinetic energies above a slightly higher threshold energy than

Table 1
Numbers of ellipsoids of different sizes that make up the fuzz structures and numbers of atoms in ellipsoids.

	20 nm	30 nm	40 nm	50 nm
number of ellipsoids	31	12	10	7
atoms in ellipsoids, solid (10^6)	25	33	65	89
W % in ellipsoids, solid	12	15	31	42
atoms in ellipsoids, hollow (10^6)	12	11	18	20

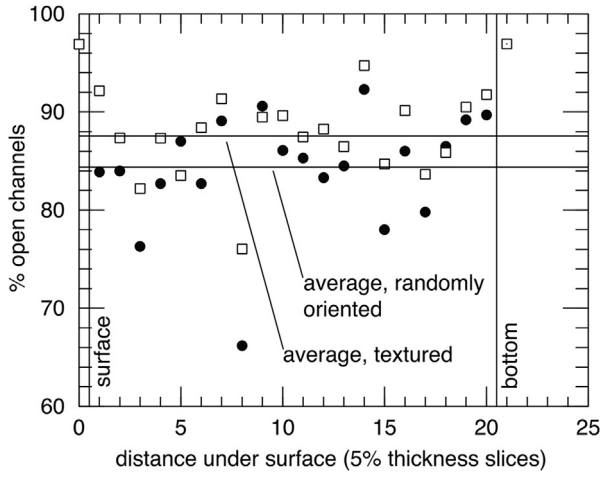

Fig. 1. The percentage of open channels in slices 1/20th the thickness of the fuzz layer. Open squares represent 3.67 vol-% textured fuzz, solid circles represent 3.67 vol-% randomly oriented fuzz. The open channels percentage for a slice is the percentage for which there are no W atoms seen along the z-direction.

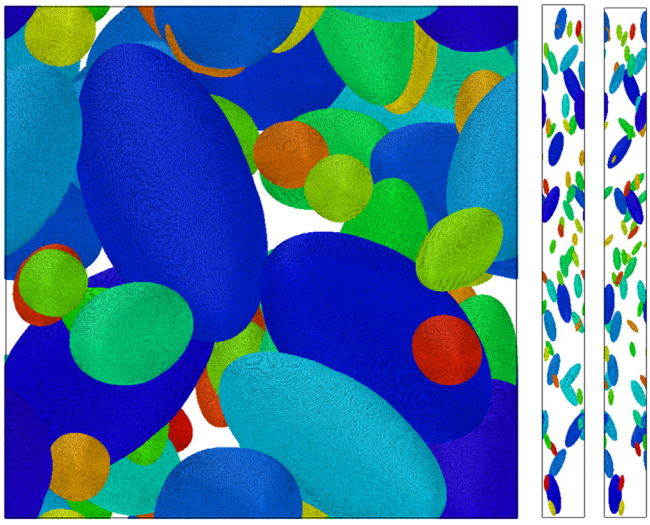

Fig. 2. Top and in-plane views of the textured 7.35 vol-% fuzz system. The in-plane dimensions are 158 × 158 nm^2, the fuzz thickness is 1.86 μm. Colours only serve to distinguish individual ellipsoids and do not correspond to any physical atomic property.

Table 2
Interatomic potentials used with their cut-off radii, as implanted in LAMMPS.

interaction	potential	cut-off radius (Å)
W-W	Ackland–Thetford, modified by Juslin-Wirth	4.40
W-He	Juslin-Wirth	3.17
He-He	Beck, with short range fit by Morishita	3.80

previously, simulations ran for more than 6 million steps for the largest, sparsest systems, requiring approximately half a year on 60 Intel Xeon cores or 96 AMD cores. He ions are subjected to a Nose-Hoover thermostat along with the W atoms, to keep the system temperature at 1500 K. While the velocity scaling factors during the simulation are all extremely close to 1 for our large systems, being subjected to a thermostat for millions of steps made He ions (unphysically) pick up or lose up to a few eV of kinetic energy while moving freely through the system. He ions were introduced every 200 MD steps rather than every 500 as previously, because the larger system volumes reduce the chances of unrealistic mid air collisions between He ions. Out of 10000 He ions introduced in each fuzz structure, a maximum of 2 were observed leaving the system with significantly increased kinetic energy, that they would have picked up from mid air collisions with other He ions. The more frequent introduction of ions into larger systems mostly cancel each other out, resulting in a similar ion flux as in our previous work of ~10^{30} m^{-2}s^{-1}. As is usual (by necessity) in MD simulations, the flux is orders of magnitude higher than in experiments. Using LAMMPS's built-in 'brick-style' subdomain algorithm provided very good load balancing, which would have been very poor for our sparse, irregularly occupied systems if a regularly spaced grid had been used. Visualisation was done using Ovito [8].

Analysis of the He trajectories was also done similar to previous work, described in appendix B of [1]. The only adjustments were an increase from 8 to 12 eV in the threshold energy of what is considered high and low ion kinetic energy for free moving atoms, and that atoms that are analysed as trapped inside a dumbbell cavity may have maximally travelled a larger distance (length of a 50 nm dumbbell cavity instead of 20 nm).

3.2. BCA calculations

The BCA algorithm has been proven to describe successfully the ballistic collisions of energetic ions with material atoms [9–11]. Recently, another BCA code, RBSADEC, was introduced in Ref. [12], which can read in xyz coordinates for an arbitrary system of atoms from an external file and simulate the slow down process of energetic ions in the described system. In RBSADEC, the conventional BCA algorithm is used to follow the trajectories of incident ions. The scattering angles of binary collisions for different impact parameters and collision energies are calculated within the universal Ziegler-Biersack-Littmark (ZBL) screened inter-atomic potential (which is also used for short interatomic distances within the Juslin-Wirth W-He MD potential) [13] using the Gauss-Mehler quadrature integration method [14]. More details about RBSADEC can be found in Ref. [12].

As in MD, one BCA calculation run consists of 10000 ion impacts. For our BCA calculations with RBSADEC we used solid versions of the fuzz systems for which hollow systems were used in MD calculations. Using solid ellipsoids allows us to do calculations with H isotopes and higher ion energies, without any of these ions penetrating the ellipsoid shells into the cavities and becoming unphysically trapped inside them. Using hundreds of millions of atoms instead of dozens of millions as in our MD simulations makes little difference for the computation time needed for the BCA calculation runs. The time required for the calculations is only weakly dependent of the number of atoms and one BCA calculation run of 10000 ion impacts takes only a few minutes on a single cpu core. Most of that time is spent reading in the coordinates file and doing initializations, the actual BCA calculation run takes less than a minute of cpu time, which is ~10 million times less than for an equivalent MD simulation. Unlike the hollow systems in MD, the solid systems were not relaxed before ion bombardment, meaning that atoms are on their lattice positions without thermal vibrations. Also, due to initially storing of coordinates for the solid systems with a limited number of digits (to keep down file sizes), the z-coordinates of atoms above 1 μm were saved with only tenths of an Å accuracy, introducing up to 0.05 Å of rounding error. However, for one fuzz system we compared ~60 eV He BCA results for the equilibrated hollow fuzz with thermal vibrations to a calculation with the equivalent solid fuzz without thermal vibrations and rounding errors in the z-coordinates of some of the atoms. Differences between

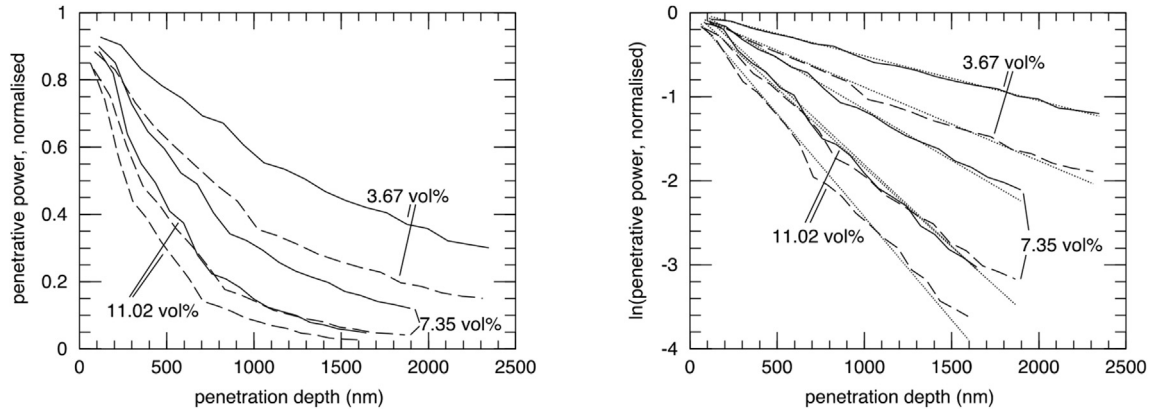

Fig. 3. Penetrative power of 60 eV He ions, impinging 0–7° off-normal on 3.67, 7.35 and 11.02 vol-% W fuzz from MD simulations. Solid lines represent textured fuzz, dashed lines represent fuzz with randomly oriented ellipsoids. Left: linear scale. Right: logarithmic scale, with exponential decay indicated by dotted lines.

the results were small.

In order to isolate the influence of parameters that were varied between calculation runs, all other settings were kept similar as much as possible. This included using the same fuzz systems for different bcc metal fuzz elements, only scaled in size by the ratio of their element lattice parameters, even though fuzz forms in somewhat different ways on different metal elements. Also, the same random number seed for the introduction of the ions was used in all calculation runs.

4. Results

4.1. MD simulations of low energy He bombardment of W fuzz

As in previous work we use 'penetrative power' as a property of ions that represents their ability to penetrate into fuzz. We use (pragmatically, other choices are possible) the kinetic energy of the He ions that

1) are freely moving, are not thermalized inside a W lattice or trapped inside a cavity
2) are moving deeper into the fuzz, rather than moving back to the vacuum
3) have 12 eV or more kinetic energy, so that the ions can still overcome the W surface barrier to penetrate into the W

Fig. 3 shows the penetrative power of He ions as a function of penetration depth into the six W fuzz structures. As in our previous work, penetrative power decreases exponentially in a fuzz structure with a roughly even W density distribution. Table 3 reports the half depths, λ.

In the simulation of the 11.02 vol-% fuzz structure with randomly oriented ellipsoids, a bug caused the atoms of two overlapping ellipsoids not to be deleted. This caused a small volume of W with twice the normal density to 'explode' at the start of the equilibration of the structure. Atoms flew out of the volume with double density with high velocities and impacted on other ellipsoids, causing them to heat up, up to 2400 K. Those ellipsoids that were completely separate from other ellipsoids remained at the higher temperature during the simulation despite the thermostat (maintaining the overall temperature at the desired value does not even out temperature differences between thermally isolated parts of the structure). The impacts from atoms followed by the high temperature caused a number ellipsoids to deform to somewhat less regular shapes. The results of BCA calculations, see next, indicate how much effect the deformed structures had on He penetration.

Table 3
Half depths λ for 60 eV He ions penetrating through W fuzz structures, determined with MD and BCA simulations. The fuzz structures in MD were hollow and atom positions included thermal vibrations. The BCA calculations were done on solid fuzz structures and atom positions did not include thermal vibrations. Because of an error in the MD simulation of the 11.02 vol-% randomly oriented structure (see text), both hollow and solid structures were calculated with BCA.

fuzz structure	λ, MD (nm)	λ, BCA (nm) [% of λ in MD]
3.67 vol-%, textured	1302	1138 [87]
3.67 vol-%, randomly oriented ellipsoids	792	710 [90]
7.35 vol-%, textured	562	488 [87]
7.35 vol-%, randomly orientated ellipsoids	364	320 [88]
11.02 vol-%, textured	358	299 [84]
11.02 vol-%, randomly oriented ellipsoids	283	solid: 207 [73] hollow: 260 [92]

4.2. Benchmarking BCA He penetration against MD results

Table 3 shows the half depths determined from BCA calculations for the solid counterparts to the hollow MD structures. Fig. 4 shows an example of penetrative power as a function of penetration depth calculated for the same structure with MD and BCA.

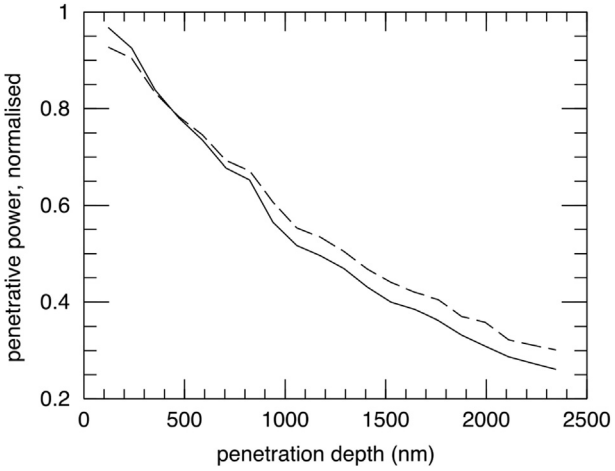

Fig. 4. Penetrative power as a function of penetration depth for 60 eV He impinging on 3.67 vol-% textured W fuzz, calculated with BCA (solid line) and MD (dashed line).

BCA half depths are systematically lower than those in MD. The largest difference is for the 11.02 vol-% randomly oriented structure, but this structure had the overlapping ellipsoids problem in the MD simulation. To compare like with like, we also did the BCA calculation run for the hollow 11.02 vol-% randomly oriented fuzz structure used in MD simulations. In that calculation run, the MD-BCA difference is comparable to the differences for other structures. If we use the result for the hollow version of the 11.02 vol-% randomly oriented structure, the BCA penetration depth is 88 ± 4% of the MD penetration depth for the six fuzz structures. Part of the difference may stem from the different interaction potentials used in the two methods, while another part may be explained by differences between MD and BCA in scattering from the ellipsoid surfaces. The relatively small MD-BCA difference shows that, despite the poor theoretical basis for the BCA at low ion energy, it produces ion penetration half depths that are reasonably accurate with a systematic underestimation of only ~12% compared to MD. This enables us to use the BCA method to quickly and computationally cheaply carry out several hundred calculation runs, in which we vary many parameters of the ion bombardment process, to see what influence each parameter has.

4.3. Varying parameters in the plasma bombardment of bcc fuzz structures

We have calculated BCA results for two different fuzz structures. The first is the 3.67 vol-% textured fuzz, which shows what the deepest ion penetration is. The second is the 7.35 vol-% fuzz with randomly oriented ellipsoids, as a structure that is rather different from the first one. Apart from the half depths being smaller for the 7.35 vol-% randomly oriented fuzz, the results were always very similar for the two structures. Hence, in the next sections only results for 3.67 vol-% textured fuzz are shown. Trends for 7.35 vol-% randomly oriented fuzz are similar, as they would probably also be for the other structures we did not calculate.

4.3.1. Varying ions species, ion mass

In a context of fusion plasma, He and H isotopes should be considered. We bombarded fuzz with both elements, varying their masses from 1 to 4 amu, i. e. we have included some non-existent isotopes. With results for the additional hypothetical isotopes we can see how the data for the existing isotopes is part of a wider trend. Also, we can see how results differ between He and H with equal mass from 1 to 4 amu. Fig. 5 shows the normalised penetrative power of different 60 eV He isotopes moving through W fuzz.

The He ion mass has only a small influence. Going from non-existent ^{1}He to ^{4}He, the half depth only decreases 8%.

Fig. 6 shows the penetrative power for H isotopes, alongside the data for He isotopes as was shown in Fig. 5.

At equal mass, He isotopes have a slightly greater half depth than H isotopes. For the naturally abundant isotopes ^{1}H and ^{4}He the H half depth is 6% larger than for He. D and T half depths are approximately equal to the ^{4}He half depth.

Since the ion mass has little influence and the half depths for D and T are approximately equal to that of ^{4}He, we only show results for ^{1}H and ^{4}He from here on.

4.3.2. Varying the fuzz element

Fig. 7 show penetrative power for 60 eV H and He ions impinging on fuzz of different elements.

The fuzz element has a greater effect on ion penetration than the ion mass or species, although the half depths for H and He on Fe are still only ~20% smaller than on W.

4.3.3. Isolating different effects of the fuzz element

The effect of the fuzz element on the half depth can be divided between the effect stemming from the different lattice parameters, different mass ratios to the ions, and different nuclear charges (and with that electron densities). The results shown in Fig. 6 suggest that the mass ratios have a very limited effect. The results in Fig. 7 further suggest that the lattice parameter is not the most important factor either, as elements with very similar lattice parameters (W and Mo) have different half depths while elements with different lattice parameters (W and Ta) have very similar half depths. This suggests that the nuclear charge (reflected in the ZBL interatomic potential, which directly depends on the charge [13]) is the most important factor. We can test the effect of different parameters by (artificially, unphysically) varying one parameter while keeping the others fixed. To test the effect of the lattice parameter, we scale the W fuzz by the lattice parameter ratio between W and Fe and between W and Ta, while keeping the atoms W with W mass. Figs. 8 and 9 show penetrative power of 60 eV He and H ions impinging on W fuzz of different sizes.

The effect of the lattice parameter on ion penetration does not exceed noise level. To see if the nuclear charge has a greater effect, we created fuzz structures of W, Ta and Fe, with masses of these elements, but all at the W lattice parameter. Figs. 10 and 11 show

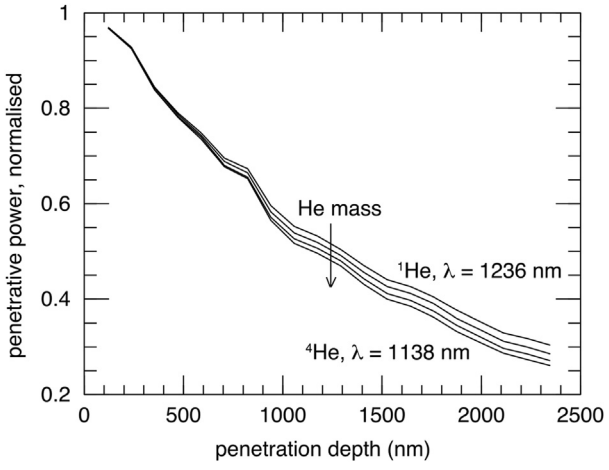

Fig. 5. Penetrative power as a function of penetration depth for 60 eV He isotopes impinging on 3.67 vol-% textured W fuzz.

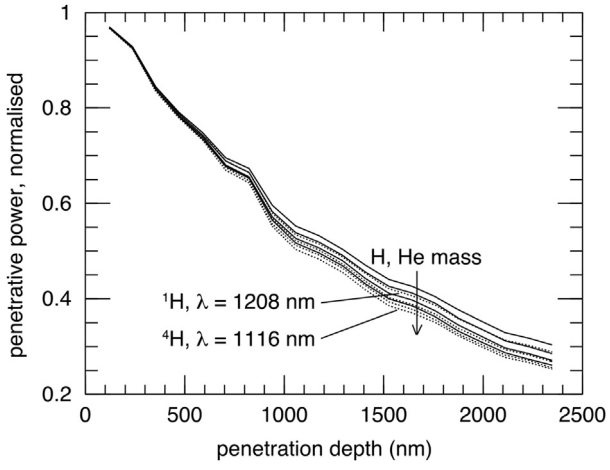

Fig. 6. Penetrative power as a function of penetration depth for 60 eV H (dotted lines) and He (solid lines) isotopes impinging on 3.67 vol-% textured W fuzz.

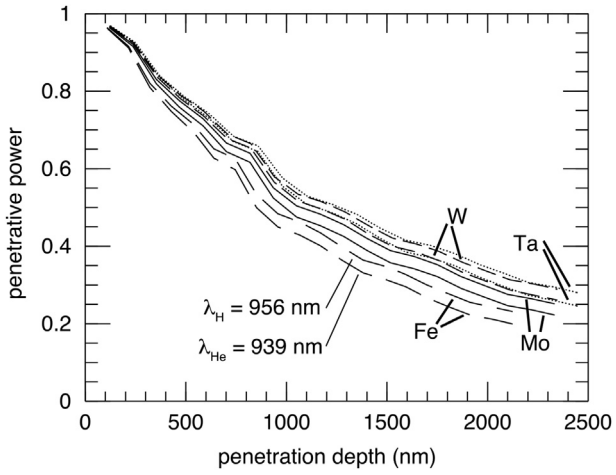

Fig. 7. Penetrative power as a function of penetration depth for 60 eV H and He impinging on 3.67 vol-% textured Ta, W, Mo, and Fe fuzz. For each fuzz element, the upper curve is for H, the bottom curve for He.

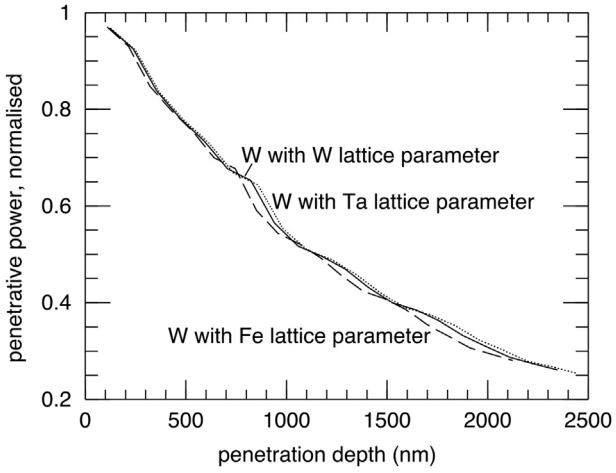

Fig. 8. Penetrative power of He as a function of penetration depth into 3.67 vol-% W textured fuzz with lattice parameters of W, Fe, and Ta.

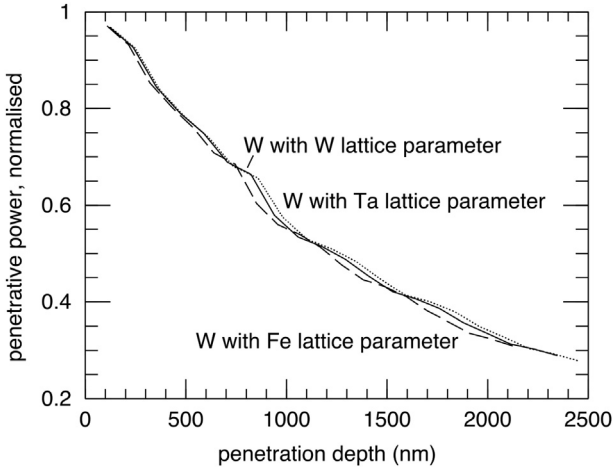

Fig. 9. Penetrative power of H as a function of penetration depth into 3.67 vol-% W textured fuzz with lattice parameters of W, Fe, and Ta.

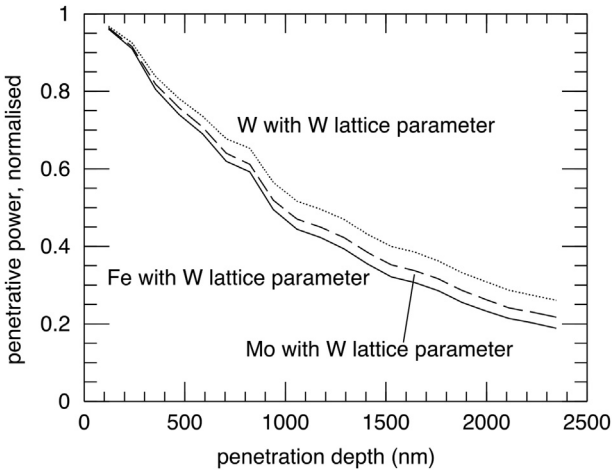

Fig. 10. Penetrative power of He as a function of penetration depth into 3.67 vol-% W, Mo, and Fe textured fuzz, all with the lattice parameter of W.

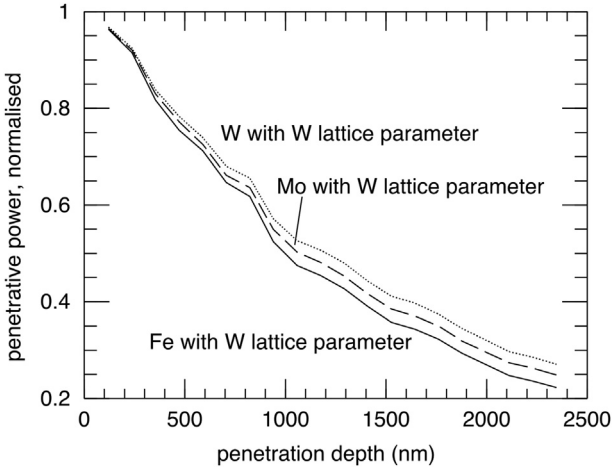

Fig. 11. Penetrative power of H as a function of penetration depth into 3.67 vol-% W, Mo, and Fe textured fuzz, all with the lattice parameter of W.

the penetrative power of He and H in W, Mo and Fe fuzz, all at the W lattice parameter.

Apart from the scaled lattice parameter, the data in Figs. 10 and 11 is very similar to the data, for both He and H, in Fig. 6. This (along with the unimportance of the ion-fuzz element mass ratio, see section 4.3.1) shows that the nuclear charge by itself mostly explains different half depths for different fuzz elements and that fuzz element mass and lattice parameter are relatively unimportant.

4.3.4. *Varying the angle of incidence*

Fig. 12 shows penetrative power as a function of penetration depth for 60 eV He and H for different angles of incidence on W fuzz.

Unsurprisingly, the angle of incidence has a big influence on ion penetration depths. Unfortunately, it is not possible to determine half depths for grazing angles of incidence, because at these angles the decay pattern is no longer exponential. For example, for the 80–87° off-normal angle, it takes ~200 nm for the normalised penetrative power to drop from 0.5 to 0.25, while it takes ~800 nm for it to drop from 0.05 to 0.025. The deviation from the exponential pattern is most likely because of the very low average kinetic energy of atoms that reach the bottom of the fuzz structure at these

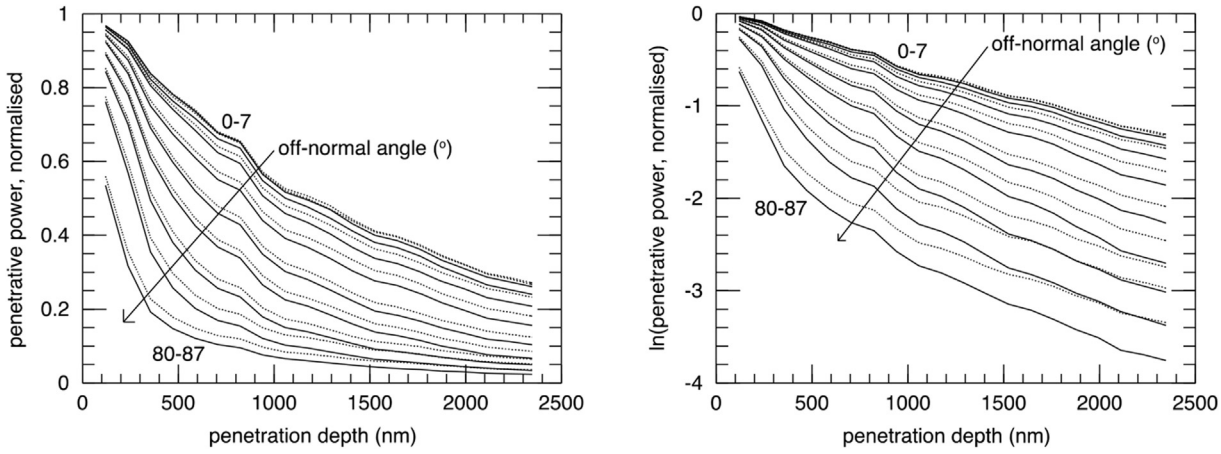

Fig. 12. Penetrative power as a function of penetration depth for 60 eV He (solid curves) and H (dashed curves) for different angles of incidence on 3.67 vol-% W textured fuzz. Left: linear scale. Right: logarithmic scale. The upper curves are for 0–7° off-normal incidence, as in all previous graphs. Curves below that are for 10–17°, 20–27°, …., 80–87° off-normal incidence.

angles. At very low energy, He and H atoms mostly just penetrate into the surface barrier a bit rather than reaching below the surface monolayer of W atoms. The atoms interact only relatively weakly with W, and for much of the time simultaneously with several W atoms at comparable distances, before being reflected. The BCA can not properly describe such low energy collisions. By contrast, Fig. 3 shows that in MD simulations, the exponential pattern does extend to lower energies.

4.3.5. Varying the ion energy

We simulated He and H ion bombardment on W and Fe substrates with energies ranging from 40 to 500 eV. Figs. 13 and 14 show the penetrative power, normalised to the initial ion energy, rather than to 1 as in previous graphs.

For He, the half depth decreases a little when raising the ion energy from 60 to 500 eV, both on W and Fe, but the decrease is within the error margin of the exponential fit. For H, the half depth increases by a few tens of %. These results show that the ion penetration behaviour is quite universal and that half depths would likely not change dramatically if the ion energy were increased by another order of magnitude.

5. Discussion

The MD results show that for the sparse W fuzz that is observed in experiments, He penetration half depths may be measured in μm. These results are based on fuzz structures that were created with several improvements over the fuzz structures in our previous work. Therefore our results provide stronger evidence for our previous suggestion that He transport through fuzz happens ballistically, rather than through diffusion through the nanorods. Given the assumptions we made in creating the fuzz structures, the outcome of our simulations still has a considerable uncertainty. For example, the choice of the numbers of ellipsoids of different sizes is a parameter that could significantly increase penetration depths further, if many of the smaller ellipsoids were merged into fewer, bigger ones. Also, in the lowest density fuzz structures, most ellipsoids are completely isolated. These structures therefore represent the correct density of objects of the approximately right size and shape for He ions to run into, but they are quite unrealistic in other respects. However, rather than suggest varying yet more parameters in the creation of fuzz structures, we will here instead reiterate our earlier recommendation to do an experimental three

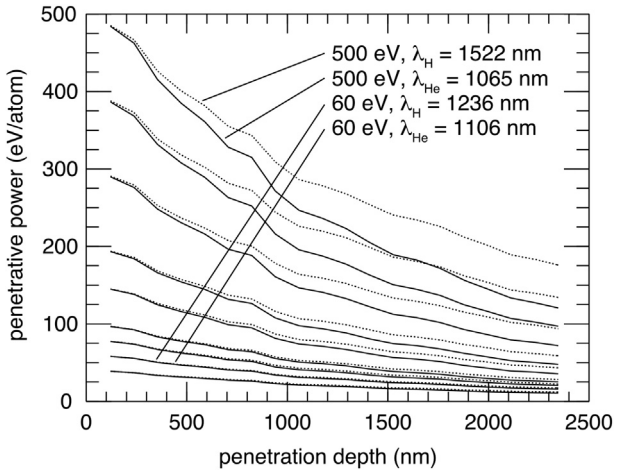

Fig. 13. Penetrative power of He (solid lines) and H (dotted lines) ions with energies of 40, 60, 80, 100, 150, 200, 300, 400, and 500 eV penetrating through 3.67 vol-% W textured fuzz.

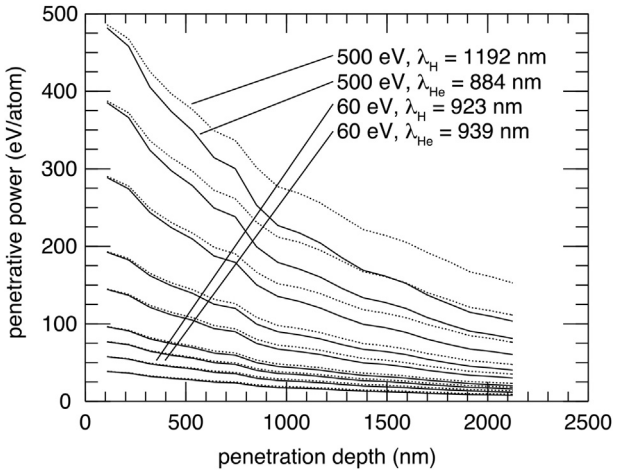

Fig. 14. Penetrative power of He (solid lines) and H (dotted lines) ions with energies of 40, 60, 80, 100, 150, 200, 300, 400, and 500 eV penetrating through 3.67 vol-% Fe textured fuzz.

dimensional structure determination of fuzz, through e.g. TEM tomography.

If, in the absence of an experimental three dimensional fuzz structure determination, further computational efforts are to be made, they need not be lengthy MD simulations. The benchmarking of BCA results against MD results shows that a simpler, 10 million times shorter calculation can produce comparable ion penetration results, with some of the MD-BCA differences in our work possibly stemming from slightly different potentials. We think the good agreement is due to three factors. 1) BCA being able to describe straight motion of ions (between collisions) just as well as the MD. 2) The repulsive interatomic potential governing ion scattering at short distances being the same in both potentials, and 3) apparently the BCA can describe also the scattering from the fuzz material surfaces well. The first 2 factors are rather obvious, but the third one is not (since BCA does not necessarily deal well with low-energy ion-surface collisions due to the lack of many-body interactions). The current simulations can be considered a confirmation that also item (3) is treated well at 60 eV. In fact, we tested lowering the ion energy from 60 eV to 20 eV, and at that lower energy BCA no longer agreed well with MD (i.e. factor 3 no longer holds). The BCA results are highly systematic, so even though absolute values for penetration depths may be underestimated, trends can still be determined very clearly.

By using the BCA methodology to determine the influence of various parameters in the ion bombardment process, we learned that for most parameters it is quite generic. The ion species (He or H), ion mass, fuzz element, and fuzz lattice parameter have at most a modest influence on ion penetration. The modest influence of the fuzz element suggests that the differences in fuzz growth on different bcc elements are caused mainly by factors other than the bombardment process, like e. g. the diffusion and clustering behaviour of He inside the different metal lattices. The lack of a strong influence of the ion/fuzz element mass ratio is perhaps somewhat surprising. We calculate the maximum energy transferred E_{tr} from an ion with energy E_0 to a fuzz atom in a binary collision with the equation

$$E_{tr} = E_0 \frac{4Mm}{(M+m)^2} \quad (1)$$

in which M and m are the masses of the fuzz element atom and the ion. For 60 eV H on W the maximum energy transfer is 1.3 eV while for 60 eV He on Fe it is 15 eV. Yet despite the maximum energy transfer for He on Fe being an order of magnitude larger than for H on W, the half depth is only 24% lower (939 vs. 1236 nm). Therefore, a mixture of He and H ions hitting a fuzz structure will remain a mixture as it penetrates through the fuzz, i. e. it will not split into deeper and less deep penetrating elements. Two parameters that did have significant influence were the angle of incidence and the ion energy. The angle of incidence is less relevant in a fusion energy context. On the surface of a fusion tokamak divertor, most of the ion energy comes from the sheath potential, which will always make the ions hit the W surface close to perpendicular. Also, while higher ion energy leads to deeper penetration, the half depths change only modestly with energy. This means that in terms of ion energy the picture is generic too. If the ion energy is doubled, one half depth into the fuzz the ion penetrative power will be comparable to that of ions hitting the outer fuzz surface with the original amount of energy. This picture can not be similarly extended to lower ion energies in our calculations, since at lower energies the BCA is less and less able to properly describe the collision processes.

While not all of the results are necessarily intuitive, a number of the results involving He (which forms fuzz, while H isotopes by themselves do not) are amenable to experimental verification. The prediction of exponentially decaying penetrative power leads to a fuzz thickness that grows with the logarithm of the ion fluence [1]. A lengthy plasma exposure run, in which the fuzz thickness is measured at different ion doses, would allow for confirmation or falsification of the idea that ion penetration is ballistic and that the penetrative power half depth is of the order of a μm. The influence of some of the parameters investigated can also be verified. If the ion half depth is more or less independent of ion energy over an order of magnitude of ion energy, then for thicker fuzz layers (where the ion flux to the bulk has become the growth limiting factor) increasing the ion energy by some factor should lead to a similar fuzz thickness if the ion flux is reduced by the same factor. Finally, if a sample is tilted halfway during a long exposure run (to change the angle of incidence from normal to strongly off-normal) this should drastically reduce the pace at which the fuzz thickness increases after tilting the sample. The aforementioned experiments would all require lengthy exposure runs that allow for the determination of fuzz thicknesses large enough to determine ion half depths from them. While previously such exposures were experimentally difficult, the recent addition of a superconductor magnet to the Magnum-PSI setup [15] allows for hours long continuous exposures of samples to high intensity, low energy ion beams. This allows for precisely the sort of experiments that can verify a number of the predictions from our calculations.

6. Summary and conclusions

We have carried out MD simulations of low energy He ion bombardment of sparse W fuzz. The goal of these simulations was to see if ion penetration depths in sparse fuzz are sufficiently large to enable the flux of He needed to grow the fuzz further 'from the bottom'. Our results show that this is the case. While we made some big assumptions in how we created the fuzz structures, these do not invalidate the important outcomes of the calculations. As was found in our previous work, ion penetration falls off exponentially with penetration depth. For the sparsest fuzz (which is observed experimentally), the penetration is measured in μm, which is sufficient to explain He transport through the thickest fuzz layers grown so far.

A recently introduced BCA code that can read in xyz coordinates for an arbitrary system of atoms was used to carry out the same ion bombardment on the same fuzz structures as in MD simulations, with 10 million times faster BCA calculations. Despite the poor theoretical justification for the BCA at low ion energies, ion penetration in the BCA calculations is on average only ~12% less deep than in MD, with some of that difference possibly being due to different interatomic potentials. The MD-BCA difference is highly systematic and trends in the results of the two methods are very similar.

We have used the possibility to carry out ion bombardment simulations at trivial computational cost to perform over 200 BCA calculation run, in which a number of parameters in the ion bombardment process were varied. The results show much of the bombardment process to be quite generic. The ion species (He or H), ion mass, fuzz element and fuzz element lattice parameter have a modest influence on ion penetration at most. An off-normal angle of incidence strongly reduces the ion penetration depth. At strongly off-normal angles of incidence, the energy of the ions that do penetrate deeply into the fuzz becomes so low that the BCA becomes highly inadequate to describe the collision processes. This is likely the reason why at low ion energies, ion penetration no longer drops off exponentially with penetration depth in BCA, while it still does so in MD. Increasing the ion energy increases the ion penetration in line with the exponential decay pattern observed at lower energies.

Acknowledgements

This work was funded by the Stichting voor Fundamenteel Onderzoek der Materie, which is financially supported by the Nederlandse Organisatie voor Wetenschappelijk Onderzoek. The work has been partly carried out within the framework of the EUROfusion Consortium and has received funding from the Euratom research and training programme 2014–2018 under grant agreement No 633053. The views and opinions expressed herein do not necessarily reflect those of the European Commission. The authors thank Barend Thijsse and Thomas Morgan for reading of the manuscript and constructive comments.

References

[1] T.P.C. Klaver, K. Nordlund, T.W. Morgan, E. Westerhof, B.J. Thijsse, M.C.M. van de Sanden, Nucl. Fusion 56 (2016) 126015.
[2] S. Takamura, N. Ohno, D. Nishijima, S. Kajita, Plasma Fusion Res. 1 (2006) 051.
[3] S. Kajita, T. Saeki, N. Yoshida, N. Ohno, A. Iwamae, Appl. Phys. Express 3 (2010) 085204.
[4] M. de Respinis, G. De Temmerman, I. Tanyeli, M.C.M. van de Sanden, R.P. Doerner, M.J. Baldwin, R. van de Krol, ACS Appl. Mater. Interfaces 5 (2013) 7621.
[5] T.J. Petty, M.J. Baldwin, M.I. Hasan, R.P. Doerner, J.W. Bradley, Nucl. Fusion 55 (2015) 093033.
[6] N. Juslin, B.D. Wirth, J. Nucl. Mater 432 (2013) 61.
[7] S. Plimpton, J. Comput. Phys. 117 (1995) 1.
[8] A. Stukowski, Model. Simul. Mater. Sci. Eng. 18 (2010) 015012.
[9] L. Bukonte, F. Djurabekova, J. Samela, K. Nordlund, S.A. Norris, M.J. Aziz, Nucl. Instr. Meth. Phys. Res. B 297 (2013) 23.
[10] M.T. Robinson, I.M. Torrens, Phys. Rev. B 9 (1974) 5008.
[11] J. F. Ziegler, J. P. Biersack, M. D. Ziegler, SRIM — The Stopping and Range of Ions in Matter, SRIM Co.
[12] S. Zhang, K. Nordlund, F. Djurabekova, Y. Zhang, G. Velisa, T.S. Wang, Phys. Rev. E 94 (2016) 043319.
[13] J.F. Ziegler, J.P. Biersack, U. Littmark, The Stopping and Range of Ions in Matter, Pergamon, New York, 1985.
[14] B. Yuan, F.C. Yu, S.M. Tang, Nucl. Instr. Meth. B 83 (1993) 413.
[15] H.J.N. van Eck, et al., Fusion Eng. Des. 89 (2014) 2150.